

Continuum Polarization Induced by Tidal Distortion in Binary Stars

J. Patrick Harrington¹

1. On the Roche Potential of Close Binary Stars

Let Ψ be the potential of a particle due to the gravitational attraction of two masses M_1 and M_2 , revolving in circular orbits about their center of mass. The separation of the masses is a , and from Kepler's third law, the angular velocity of the revolution about the center of mass, ω , is $\omega^2 = G(M_1 + M_2)/a^3$. We assume the particle is rotating at the same angular velocity ω , so that the potential must also include the centrifugal force. The centrifugal term due to the rotation is $-\frac{1}{2}\omega^2 R_*^2$, where R_* is the distance from the axis of rotation. We adopt a coordinate system with the origin at M_1 and the x-axis along the line to M_2 . Let the mass ratio be $q = M_2/M_1$. The location of the center of mass, also on the x-axis is $X_{cm} = aM_2/(M_1 + M_2) = a q/(1 + q)$. The system revolves about the center of mass, and we chose the z-axis to be parallel to the axis of rotation.

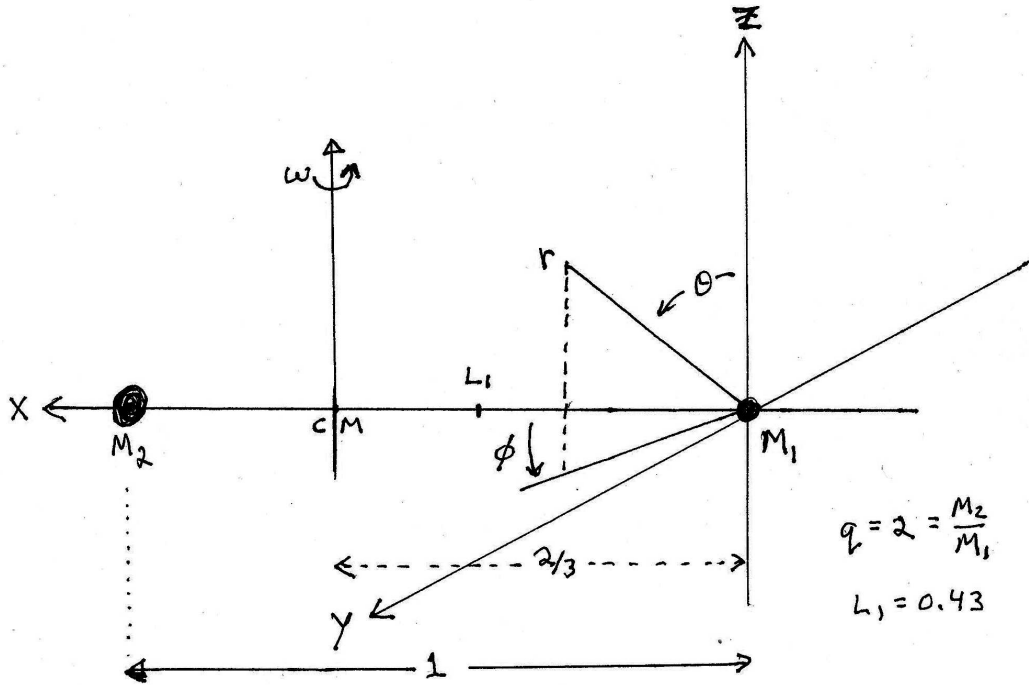


Fig. 1.— The coordinate system a binary pair.

The potential energy per unit mass of a particle is then

$$\Psi = -\frac{GM_1}{R_1} - \frac{GM_2}{R_2} - \frac{1}{2} \frac{G(M_1 + M_2)}{a^3} R_*^2, \quad (1)$$

¹Department of Astronomy, University of Maryland, College Park, MD

where R_1 and R_2 are the distances of our point at (X, Y, Z) from M_1 and M_2 , respectively. We will adopt the separation a as our unit of length, and we write $R_1/a = r$, $R_2/a = r'$ and $R_*/a = r_*$. Also $X/a = x$, $Y/a = y$ and $Z/a = z$. Then

$$a \Psi = -\frac{GM_1}{r} - \frac{GM_2}{r'} - \frac{1}{2}G(M_1 + M_2) r_*^2 . \quad (2)$$

We then can introduce a dimensionless potential Ω defined by

$$\Omega = -\frac{2a}{G(M_1 + M_2)} \Psi . \quad (3)$$

The distance from any point (x, y, z) to M_1 (the origin of our coordinate system) is

$$r = \sqrt{x^2 + y^2 + z^2} , \quad (4)$$

while the distance to M_2 , located at $(1,0,0)$, is

$$r' = \sqrt{(1-x)^2 + y^2 + z^2} . \quad (5)$$

Then Ω becomes

$$\Omega = \frac{2}{1+q} \frac{1}{r} + \frac{2q}{1+q} \frac{1}{r'} + (x - x_{cm})^2 + y^2 , \quad (6)$$

where $x_{cm} = q/(1+q)$.

The gradient of the potential in Cartesian coordinates is

$$\nabla\Omega = \frac{\partial\Omega}{\partial x} \hat{\mathbf{i}} + \frac{\partial\Omega}{\partial y} \hat{\mathbf{j}} + \frac{\partial\Omega}{\partial z} \hat{\mathbf{k}} \quad (7)$$

Taking the derivatives we find the components of the gradient:

$$\frac{\partial\Omega}{\partial x} = \frac{2}{1+q} \left(\frac{-x}{r^3} \right) + \frac{2q}{1+q} \left(\frac{1-x}{(r')^3} \right) + 2 \left(x - \frac{q}{1+q} \right) \quad (8)$$

$$\frac{\partial\Omega}{\partial y} = \frac{2}{1+q} \left(\frac{-y}{r^3} \right) + \frac{2q}{1+q} \left(\frac{-y}{(r')^3} \right) + 2y \quad (9)$$

$$\frac{\partial\Omega}{\partial z} = \frac{2}{1+q} \left(\frac{-z}{r^3} \right) + \frac{2q}{1+q} \left(\frac{-z}{(r')^3} \right) \quad (10)$$

We may also examine a spherical coordinate system. The relationships to xyz coordinates are

$$x = r \sin \theta \cos \phi \quad y = r \sin \theta \sin \phi \quad z = r \cos \theta \quad (11)$$

Substituting into eqn (5), we find

$$r' = \sqrt{r^2 - 2r\lambda + 1} \quad \text{where} \quad \lambda = \sin \theta \cos \phi . \quad (12)$$

The remaining terms of eqn (6) are

$$(x - x_{cm})^2 + y^2 = (r \sin \theta \cos \phi - x_{cm})^2 + (r \sin \theta \sin \phi)^2 = r^2 \sin^2 \theta - 2r\lambda x_{cm} + x_{cm}^2 , \quad (13)$$

and we recall that $x_{cm} = q/(1+q)$. Gathering these terms, the expression for the potential in spherical coordinates is

$$\Omega = \frac{2}{1+q} \frac{1}{r} + \frac{2q}{1+q} \left\{ \frac{1}{\sqrt{1-2r\lambda+r^2}} - r\lambda \right\} + r^2 \sin^2 \theta + \left(\frac{q}{1+q} \right)^2 \quad (14)$$

As the last term is a constant, it is often omitted. We retain it so our values of Ω will agree in both coordinates.

In spherical coordinates, the gradient of the potential is

$$\nabla \Omega = \frac{\partial \Omega}{\partial r} \hat{\mathbf{r}} + \frac{1}{r} \frac{\partial \Omega}{\partial \theta} \hat{\boldsymbol{\theta}} + \frac{1}{r \sin \theta} \frac{\partial \Omega}{\partial \phi} \hat{\boldsymbol{\phi}} \quad (15)$$

Differentiating, we obtain the components of the gradient:

$$\frac{\partial \Omega}{\partial r} = \frac{2}{1+q} \left(\frac{-1}{r^2} \right) + \frac{2q}{1+q} \left\{ \frac{\lambda - r}{(1-2r\lambda+r^2)^{3/2}} - \lambda \right\} + 2r \sin^2 \theta \quad (16)$$

$$\frac{1}{r} \frac{\partial \Omega}{\partial \theta} = \frac{2q}{1+q} \left\{ \frac{\cos \theta \cos \phi}{(1-2r\lambda+r^2)^{3/2}} - \cos \theta \cos \phi \right\} + 2r \sin \theta \cos \theta \quad (17)$$

and with $d\lambda/d\phi = -\sin \theta \sin \phi$,

$$\frac{1}{r \sin \theta} \frac{\partial \Omega}{\partial \phi} = \frac{2q}{1+q} \left\{ 1 - \frac{1}{(1-2r\lambda+r^2)^{3/2}} \right\} \sin \phi \quad (18)$$

The inner Lagrangian point, L_1 , is located on the x-axis in the (0,1) interval. We can obtain the location of this point for a given mass ratio q by solving the equation $\partial \Omega / \partial x = 0$. Looking at eqn (8), we see that for $y = z = 0$, $r^3 = x^3$ and $(r')^3 = (1-x)^3$. After multiplication by $(1+q)/2$, we obtain

$$\frac{q}{(1-x)^2} - \frac{1}{x^2} + (1+q)x - q = 0 \quad (19)$$

This 5th order equation in x does not have an algebraic solution, but it is easily solved numerically. Note that we could also use eqn (16) and set $\partial \Omega / \partial r = 0$. To do this, note that on the x-axis, $\lambda = 1$ and the term in braces becomes

$$\left\{ \frac{1-r}{(1-r)^3} - 1 \right\}, \quad (20)$$

and, with $\sin^2 \theta = 1$, we obtain the same equation for r as eqn (19) for x . The Roche lobes are defined by the surface of constant potential which passes through the L_1 . If we evaluate eqn (6) on the x-axis for the point $(L_1, 0, 0)$ we have

$$\Omega(L_1) = \left(\frac{2}{1+q} \right) \frac{1}{L_1} + \left(\frac{2q}{1+q} \right) \frac{1}{1-L_1} + \left(L_1 - \frac{q}{1+q} \right)^2 \quad (21)$$

Thus for a given q , we may solve eqn (19) for the location of the Lagrange point L_1 , using any numerical root solver (such as Brent's method). Then eqn (21) provides the value

of the potential for the Roche lobe. To find the radius of the lobe for any (θ, ϕ) pair, we insert this potential into eqn (14) to obtain an equation for r , which we may again solve by Brent’s method. Once we have $r(\theta, \phi)$, we can use eqns (8-10) to evaluate $-\nabla\Omega$, which is just the effective gravity at this point. In Table 1 we give a few values for q in the range 0.3-3.0.

Table 1: **Parameters for Roche lobes of various q**

$q = M_2/M_1$	r at L1	Ω (L1)	r at L2	$ \nabla\Omega(L2) $
0.3	0.62087	3.8475	0.5151	4.5065
0.5	0.57075	3.9456	0.4679	4.7961
0.8	0.52295	3.9942	0.4250	4.8508
1.0	0.5	4.0	0.4050	4.7939
1.2	0.48124	3.9961	0.3889	4.7079
1.5	0.45838	3.9809	0.3696	4.5577
2.0	0.42925	3.9456	0.3454	4.3017
3.0	0.38926	3.8707	0.3128	3.8554

Stars which do not fill the Roche lobe will assume a shape that will correspond to values of $r(\theta, \phi)$ obtained by solving eqn (14) using a value of Ω larger than that obtained from eqn (21). We are thus able to obtain the shape and effective surface gravity of any star in a binary system, to the extent that the gravitational potential of the stars can be approximated by that of a point mass.

As a star in a close binary system evolves, it will generally expand, the surface following successive equipotentials, until it reaches the critical $\Omega(L_1)$, at which point mass transfer to the companion may occur. We will be interested in the variations in the flux and polarization of radiation of stars with substantial distortion, i.e., stars filling potential surfaces near $\Omega(L_1)$. The surfaces just inside the critical surface correspond to slightly larger values of Ω . See Fig. 2.

To evaluate the radiation from the binary, we also need the surface temperature at each (θ, ϕ) point. The earliest attempt to solve this problem resulted in the von Zeipel (1924) “law”, which states that the flux from the surface should be proportional to the local effective gravity so that $T_{eff} \propto g_{eff}^{1/4}$. Subsequent work suggested that while the von Zeipel law may be nearly correct for stars with radiative envelopes, it was not justified for stars with convective envelopes. Lucy (1967) found that for convective stars $T_{eff} \propto g_{eff}^{0.08}$. However, more recent work by Espinosa Lara and Rieutord (2012) concludes that exponent varies in the range 0.20-0.25. We will thus adopt the von Zeipel exponent of 0.25.

1.1. Polarization from Distorted Binaries

Radiation emerging from stellar atmospheres is generally slightly polarized especially for hot or cool stars. Due to the spherical symmetry of most stars, this polarization cancels out for a distant observer. The tidal and centrifugal distortion of a star in a close binary

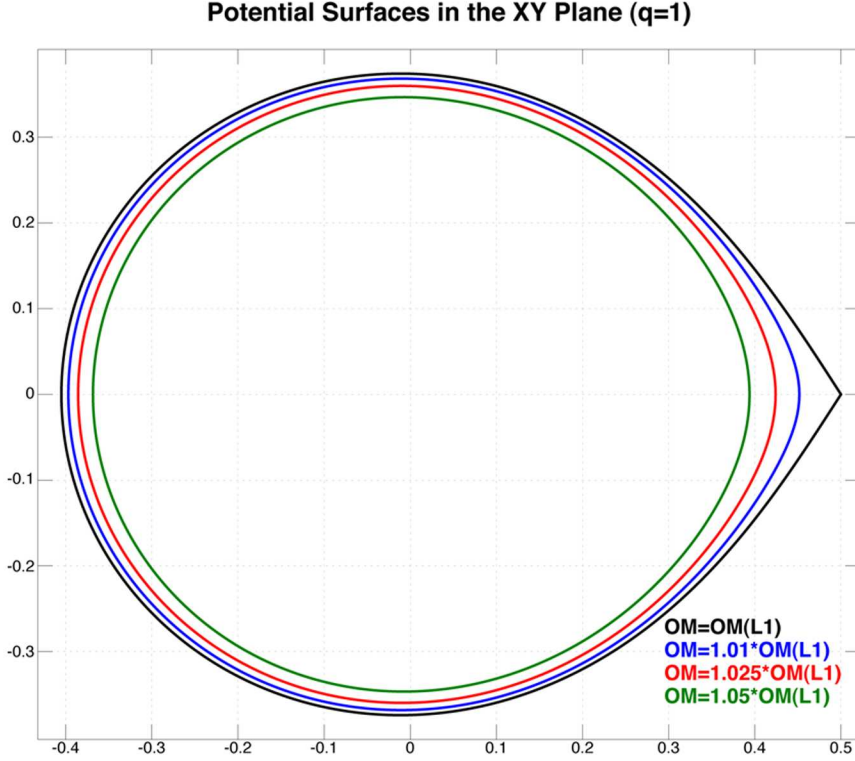


Fig. 2.— Some potential surfaces in the xy plane for a mass-ratio of $q = 1$. The critical surface passing through the Lagrange point L_1 is $\Omega(L_1)$ [labeled $OM(L_1)$]. Higher values of Ω (corresponding to more negative Ψ) give surfaces inside the critical lobe. We show surfaces corresponding to 1.01, 1.025 and 1.05 $\times \Omega(L_1)$.

system brakes the symmetry. We will evaluate the net polarization to be expected in such situations.

We first consider the simplest case where we view the star (assumed corotating) in the plane of the orbit - the x - y plane. We integrate the emergent radiation over the visible surface as seen from all ϕ_0 angles from 0 to π . The most direct way to do this is to cover the entire star with elements of area dA and then calculate μ , the cosine of the angle between the normal to the stellar surface and line of sight. We then zero out all regions where $\mu < 0$. The vector towards the observer is $\hat{o} = (\cos \phi_0)\hat{x} + (\sin \phi_0)\hat{y}$, where ϕ_0 is the phase angle of the viewer. The normal to the equipotential surface is $\hat{n} = -\vec{g}_{eff}/|g_{eff}|$, where $\vec{g}_{eff} = \nabla\Omega$. Then $\mu = \hat{o} \cdot \hat{n}$. The surface normal, \hat{n} , will not generally be parallel to the radial vector \hat{r} . Let γ be the angle between the two vectors; then $\cos \gamma = \hat{r} \cdot \hat{n}$. The element of surface area is $dA = 2\pi r^2 (\sin \theta / \cos \gamma) d\theta d\phi$, where the factor $1/(\cos \gamma)$ accounts for the increase in the element of area dA to the extent that it is inclined to \hat{r} . The flux from the binary component M_1 viewed from phase angle ϕ_0 in the orbital plane is given by

$$I(\phi_0) = \int I(\mu) \mu dA \quad (22)$$

where $I(\mu)$ is the intensity emerging at angle $\cos^{-1} \mu$ with respect to the normal to the

surface, μ is a function of θ, ϕ and ϕ_0 , and $I(\mu)$ must take into account the von Zeipel variation of the total flux with effective surface gravity.

To evaluate the net polarization, we integrate the Stokes parameter $Q(\mu)$. (We need not consider the Stokes U , as it will cancel out by symmetry.) To do this, we need to take the emergent $Q(\mu)$, which is referenced to the local normal \hat{n} and rotate it so it is referred to the z-axis. This will involve a rotation through an angle ξ , which is the angle between the projection of \hat{n} on the plane perpendicular to \hat{o} and the z-axis. If we first rotate \hat{n} about the z-axis by $-\phi_0$, so the new y-z plane is the plane of the sky, then ξ is the arctan of the new y-component of \hat{n} divided by the z-component. The net Stokes parameter is then given by

$$Q(\phi_0) = \int Q(\mu) \cos(2\xi) \mu dA \quad (23)$$

We first look at the classic (but unrealistic) case of a pure electron-scattering atmosphere as solved originally by Chandrasekhar (1960). To get the largest effect, we assume the star nearly fills the Roche lobe: we use a potential surface slightly higher (inside of) the critical surface: $\Omega = 1.01 \Omega(L_1)$. Fig. 3 shows results for three values of the mass ratio q .

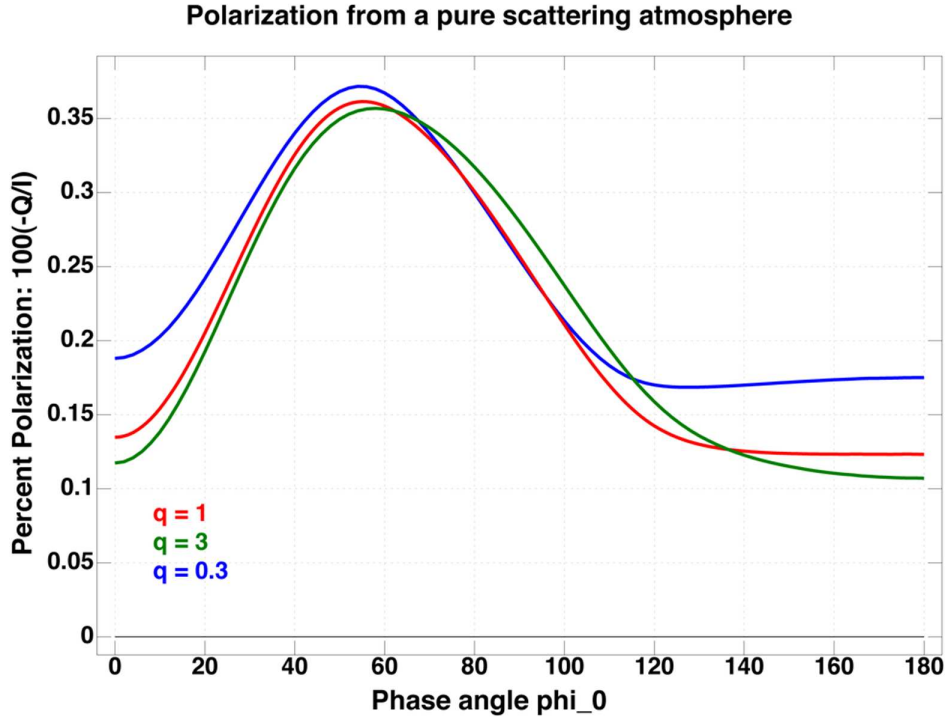


Fig. 3.— The polarization for a pure electron-scattering atmosphere for three values of $q = M_2/M_1$. The potential surface is $1.01 \Omega(L_1)$. The polarization is negative, i.e., perpendicular to the z-axis.

While we have considered the changing magnitude of the polarization as viewed in the plane of the orbit, it is also easy to compute the polarization as seen along the z-axis. From this viewpoint the magnitude of the polarization is constant, but the angle of the polarization will rotate twice through 180° during one orbital period. For this calculation we just make $\hat{o} = \hat{z}$. For pure electron scattering, assuming $\Omega = 1.01\Omega(L_1)$, the percentage polarization is

0.0896, 0.142, and 0.182 for mass ratios $q = 0.3, 1,$ and $3,$ respectively.

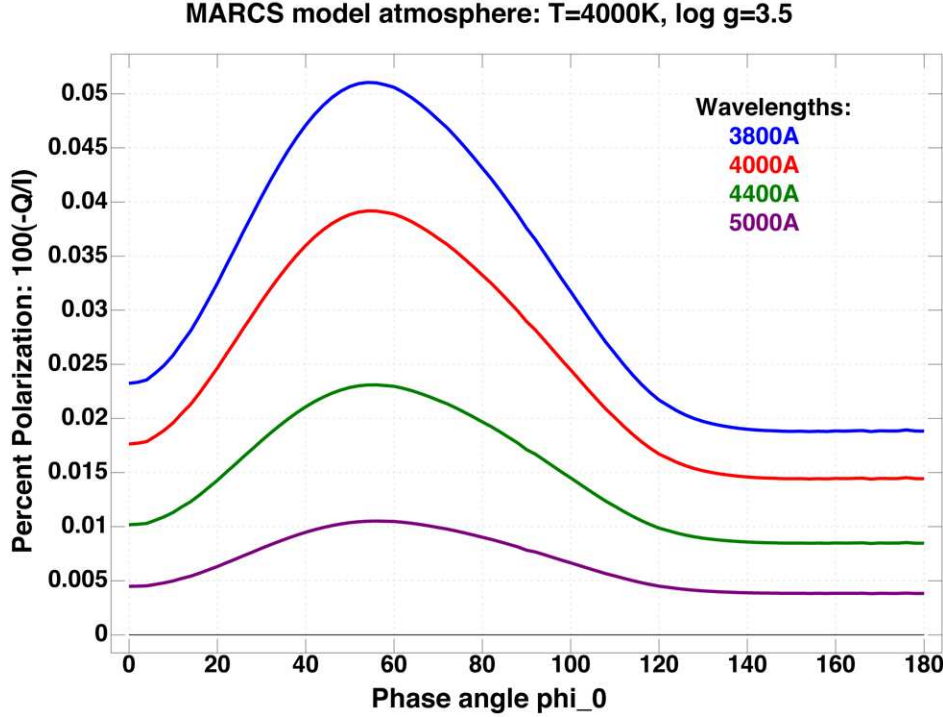


Fig. 4.— The polarization for a MARCS stellar atmosphere. Results are shown for four wavelengths. The potential surface is $1.01 \Omega(L_1)$.

For a more realistic estimate of this effect, we have made use of the $I(\mu)$ and $Q(\mu)$ Stokes parameters from a MARCS stellar atmosphere model with $T = 4000\text{K}$ and $\log g = 3.5$, with solar abundances. A careful calculation would take into account the changing surface temperature and gravity over the star. However, for this estimate, we have simply scaled the magnitude of I and Q from each point according to von Zeipel’s relation: $I, Q \propto g_{eff}$. The results are shown in Fig. 4. We see that the maximum change in polarization during the cycle is no more than $\sim 0.03\%$. As viewed along the z-axis, the amplitude of the rotating polarization is 0.0201, 0.0156, 0.00927 and 0.00429 for wavelengths of 3800, 4000, 4400 and 5000Å, respectively.

When the star is viewed from an arbitrary angle other than the orbital plane (inclination $= 90^\circ$) or along the z-axis (inclination $= 0^\circ$), the results are more complicated, as both the magnitude and angle of the polarization will vary with phase. In this case, we must consider the Stokes U parameter, which will arise when we rotate the frame of reference from the vector normal to the element of the stellar surface to the direction of the projected z-axis. The integrated U is given by an equation similar to eqn (23):

$$U(\phi_0) = \int U(\mu) \sin(2\xi) \mu dA , \quad (24)$$

where now to obtain the angle ξ , we must, in addition to rotating the normal vector \hat{n} about the z-axis by $-\phi_0$, rotate about the new y-axis by $\pi/2 - inc$, where inc is the angle

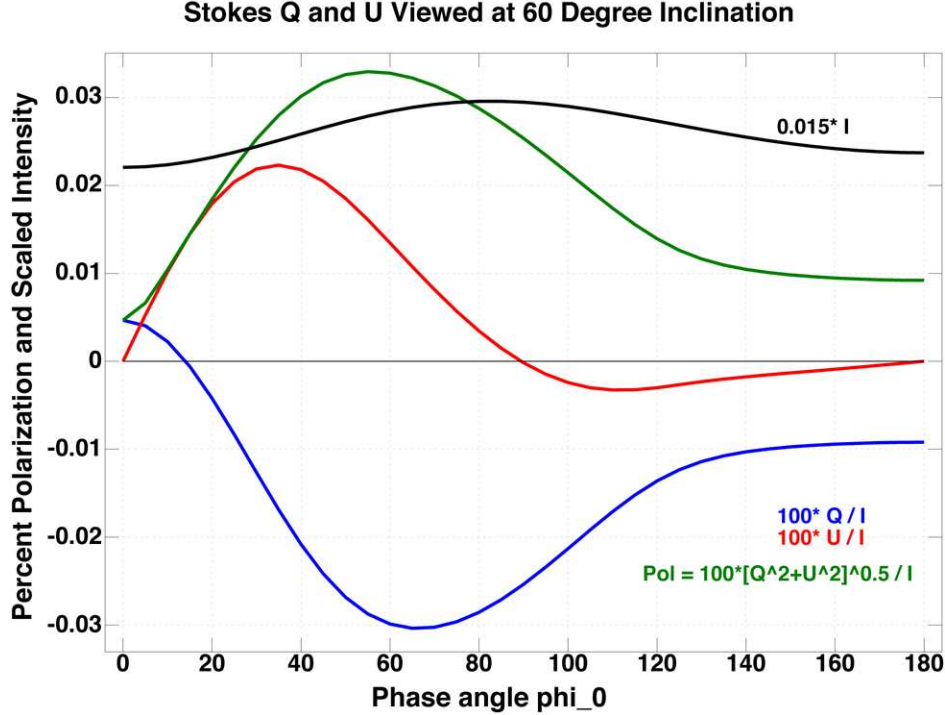


Fig. 5.— Polarization as a function of phase angle for a viewing inclination of 60° . We show the variation of the Stokes Q (blue) and U (red) as percent of the total intensity I , while the magnitude of the polarization, $P = 100 \times \sqrt{Q^2 + U^2}/I$, is the green curve. The black curve is the total intensity I , scaled to fit the plot. This is for a 4000K, $\log g = 3.5$ MARCS stellar atmosphere at 4000\AA . As before, the potential surface is $1.01 \Omega(L_1)$.

between the line-of-sight and the z -axis. Just to give an indication of the effects predicted, we present some results for the case considered above: $T = 4000\text{K}$ and $\log g = 3.5$, at a wavelength of 4000\AA . In Fig. 5 we show how the Stokes Q and U vary with phase. We can find the angle of the polarization (w.r.t. the z -axis) from $\chi = (1/2) \arctan(U/Q)$.

In Figs. 6 and 7 we show how the amplitude of the polarization varies with phase for 11 different angles. In Fig. 7 it is interesting to note that for $inc = 65^\circ$ the polarization drops to nearly zero for a phase angle of 0° , i.e. viewed in the x - z plane.

We have also done a few calculations for hot stars, using the TLUSTY model atmospheres with solar abundances. We show some results in Figs. 8 and 9. Here we have considered a viewing angle of $inc = 75^\circ$; the results do not differ much from the view in the orbital plane. The polarization can be relatively large in the (unobservable!) far UV, but is very small in the visible. This is in general true for hot atmospheres.

These calculations are for the single component of a binary system. *They do not take into account the transit of the companion or eclipse of it.* If the companion star is nearly spherical (i.e., not near its critical Roche surface), such geometrical effects would not be hard to compute. However, we have only considered gravity darkening, while the companion

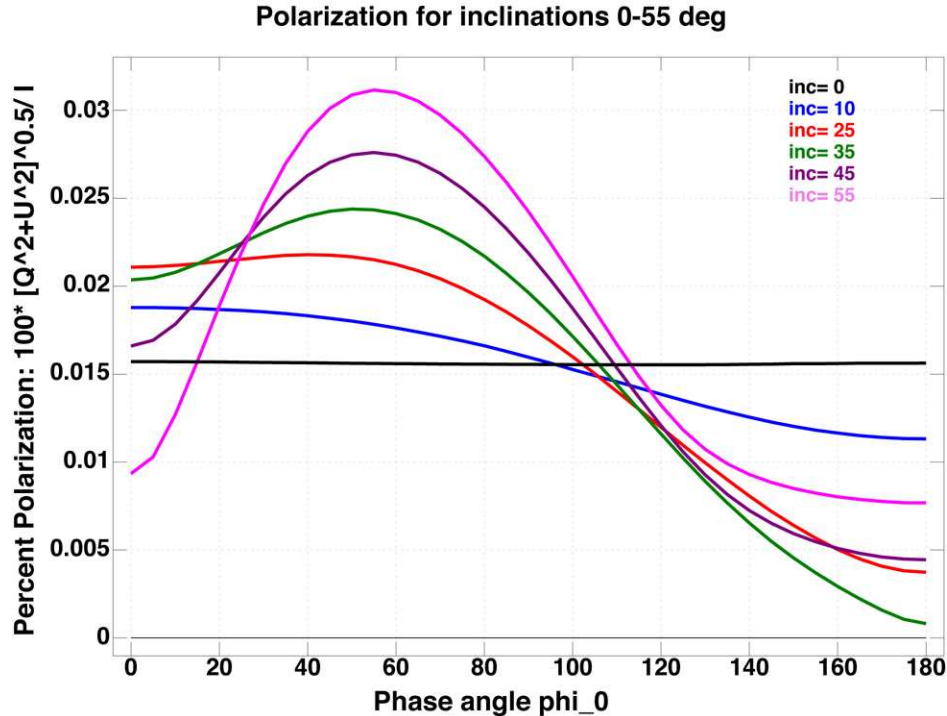


Fig. 6.— The magnitude of the polarization as a function of phase angle as seen from six angles of inclination between 0° and 55° . At 0° we are looking perpendicular to the orbital plane and the magnitude of the polarization remains constant, while the angle rotates. As the inclination increases, the variation in magnitude of the polarization increases. As above, we use a $T=4000\text{K}$, $\log g = 3.5$ MARCS stellar atmosphere at 4000\AA ; the potential surface is $1.01 \Omega(L_1)$.

could illuminate the star's atmosphere and thus change the distribution of flux over the surface as well as the structure of the atmosphere and hence the polarization of the emergent radiation. While this could also be an interesting effect, in view of the small amplitudes seen in Fig. 4, it does not seem worthwhile to pursue this further. Indeed, in a binary system where one of the stars is near the critical surface, we expect material to escape the stellar atmosphere and this circumstellar material will give rise to larger polarization effects not contemplated in these models.

5 December 2016

2. References

- Chandrasekhar 1960, "Radiative Transfer", p 248, Dover
 Espinosa Lara, F. and Rieutord, M. 2012, A.&A, 547, A32.
 Lucy, L. B. 1967, Z. Astrophys, 65, 89.
 von Zeipel, H. 1924, MNRAS, 84, 665.

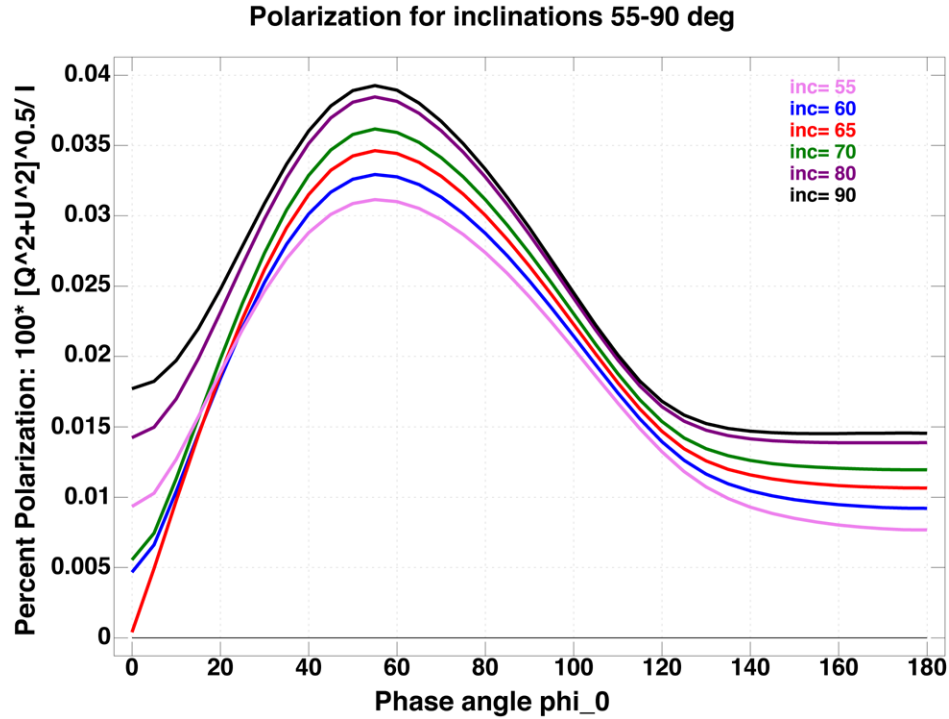


Fig. 7.— The magnitude of the polarization as a function of phase angle as seen from six angles of inclination between 55° and 90° . At 90° we are looking in the orbital plane and we obtain the red curve of Fig. 4. As above, we use a $T=4000\text{K}$, $\log g = 3.5$ MARCS stellar atmosphere at 4000\AA .

P.S. The code used for these computations can be found at
<http://www.astro.umd.edu/~jph/Binary.ijs> (pure electron scattering)
<http://www.astro.umd.edu/~jph/BinA.ijs> (cool star atmospheres)
<http://www.astro.umd.edu/~jph/BinB.ijs> (hot star atmospheres)

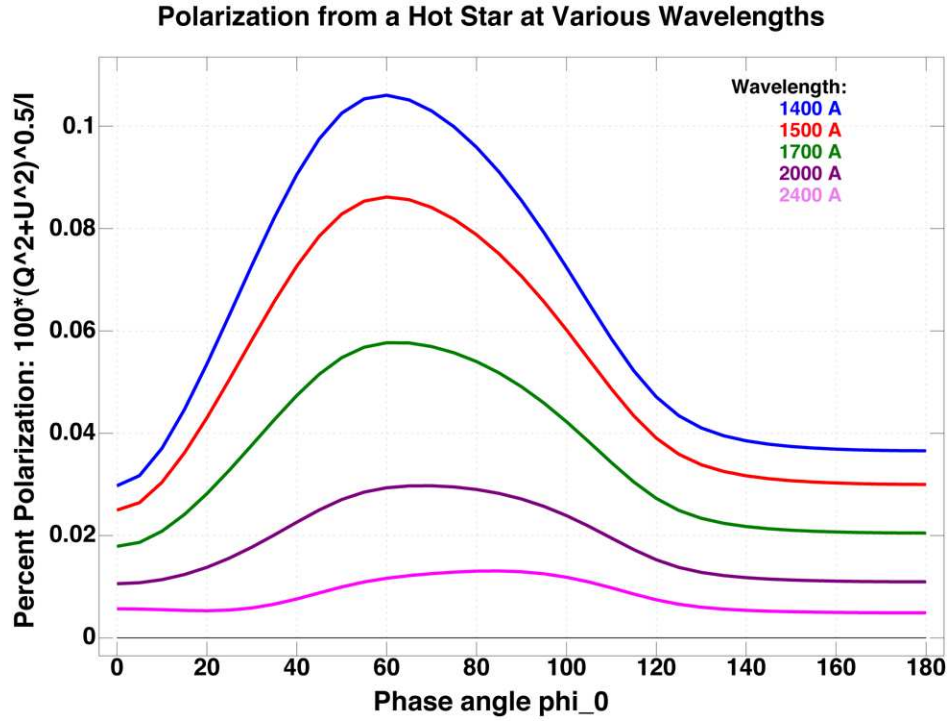


Fig. 8.— The percentage of polarization for wavelengths between 1400Å and 2400Å. This is for a star with $T=30,000\text{K}$ and $\log g=4.0$, seen an angle of $inc = 75^\circ$. Again, the potential surface is $1.01 \Omega(L_1)$.

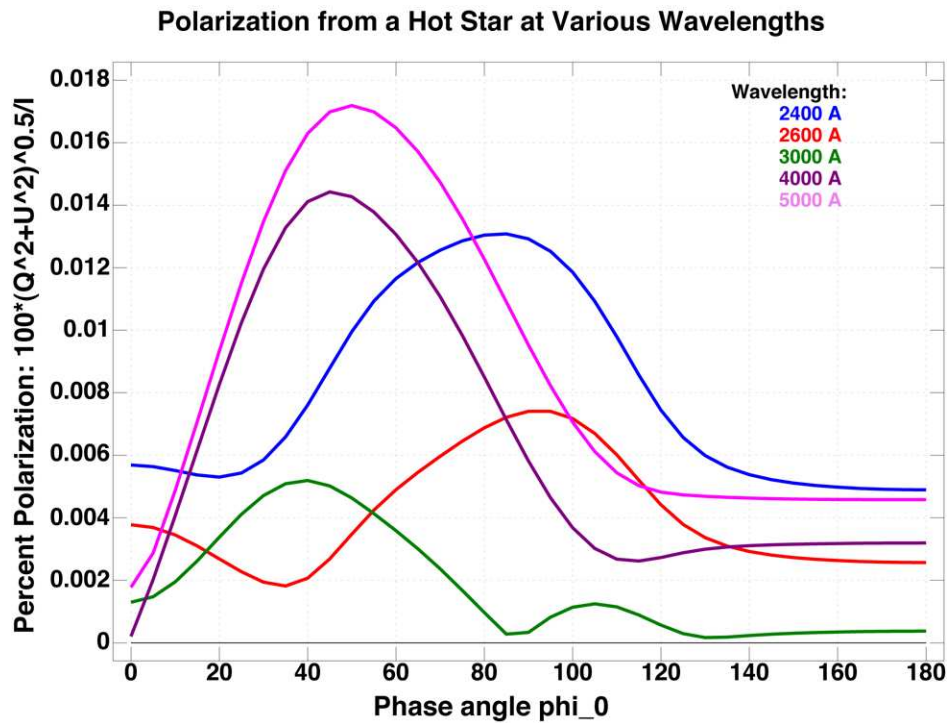


Fig. 9.— The percentage of polarization for wavelengths between 2400Å and 5000Å. As in Fig. 8, $T=30,000\text{K}$ and $\log g=4.0$, and the star is seen an angle of $inc = 75^\circ$. At these wavelengths, the behavior is more complex.

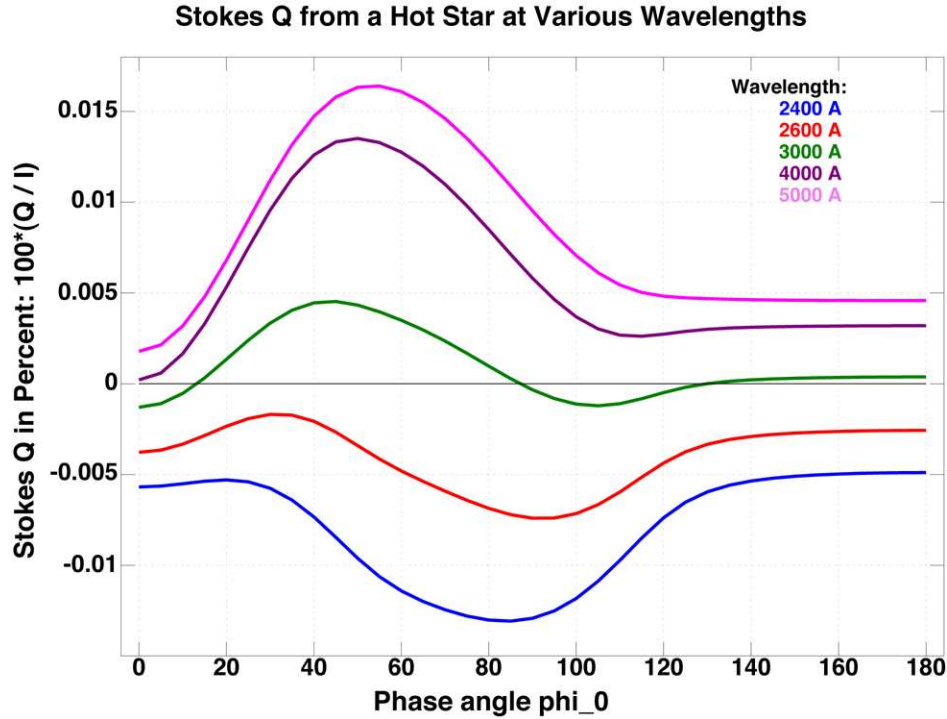


Fig. 10.— Here we plot the Stokes Q parameter for the same star as in Figs. 8 and 9, for wavelengths between 2400\AA and 5000\AA . We see that in the UV, Q is negative (polarization perpendicular to the z -axis), while in the visible, Q is positive (polarization parallel to the z -axis). The cross over occurs around 3000\AA for this atmosphere. This is because the sense of the polarization is determined by the poles (large $|z|$) which do not experience the equatorial gravity darkening. For hot stars, the emergent radiation is polarized parallel to the surface of the atmosphere in the UV, but switches to polarization perpendicular to the surface in the visible.